

Diazosulfonate Polymer Complexes: Structure and Wettability

Andreas F. Thünemann,^{*,†,||} Ute Schnöller,[‡] Oskar Nuyken,[‡] and Brigitte Voit[§]

Max Planck Institute of Colloids and Interfaces, Am Mühlenberg, 14476 Golm, Germany; Lehrstuhl für Makromolekulare Stoffe, Technische Universität München, Lichtenbergstrasse 4, 85747 München, Germany; Institut für Polymerforschung Dresden, Hohe Strasse 6, 01069 Dresden, Germany; and Institute of Theoretical Physics, Heinrich Heine University Düsseldorf, Universitätssrass 1, D-40225 Düsseldorf, Germany

Received February 4, 2000; Revised Manuscript Received April 27, 2000

ABSTRACT: Polymeric complexes were prepared by using acrylate based copolymers, which contained 20, 30, 50, and 100 mol % diazosulfonate groups and a commercially available fluorinated surfactant (Fluorad FC135). The glass transition temperatures of the complexes were determined to be 71 ± 3 °C, this was independent of the amount of diazogroups. All these complexes are stable up to temperatures of about 200 °C. As determined by wide- and small-angle X-ray diffraction, the solid states of the complexes in the bulk material were determined to be smectic A-like structures with long periods of 3.8–4.4 nm. Ultrathin films with thicknesses in the range 4–40 nm were prepared by spin coating. The wetting behavior of the films was found to be independent of their thickness. As determined by automatic drop shape analysis of the contact angle measurements, the surface energies of complex films were in the range 10–14 mN/m.

Introduction

A number of interesting self-organizing supramolecular structures have already been described and proposed as promising for the development of smart materials.¹ They originate from the complexation of polyelectrolytes with ionic amphiphiles such as fluorinated surfactants.² The simplicity of their synthesis and the variability of these mesomorphous materials are attractive features which simplify the “fine-tuning” of the resultant structures.^{3,4} Recently we described the structural and physical properties of polyelectrolyte fluorinated surfactant complexes (PEFA).⁵ The combination of well-ordered supramolecular structures, low surface energies, and adjustable tribological properties make PEFA unique polymeric materials, which are of fundamental as well as of industrial interest. For example, products produced from PEFA have been put on the market as dirt repellent and low friction coatings.⁶ It was shown earlier that polyelectrolytes containing diazosulfonate chromophores are useful for the preparation of solid polyelectrolyte surfactant complexes.^{7,8}

In the present work we report on the thermal properties, the structures, and the wetting characteristics of complexes of anionic diazosulfonate polymers and a commercially available fluorinated cationic surfactant (Fluorad FC135). The charge density of the polymers is in the range 20–100 mol %.

Experimental Section

Materials. The diazosulfonate containing acrylamido-4-phenyldiazosulfonate **M** (see Figure 1 for polymers) was prepared, in analogy to the procedure described earlier,⁹ by combining 4-aminophenyldiazosulfonate with acryloyl chloride. Acrylic acid (Fluka) and methyl methacrylate (Fluka) were

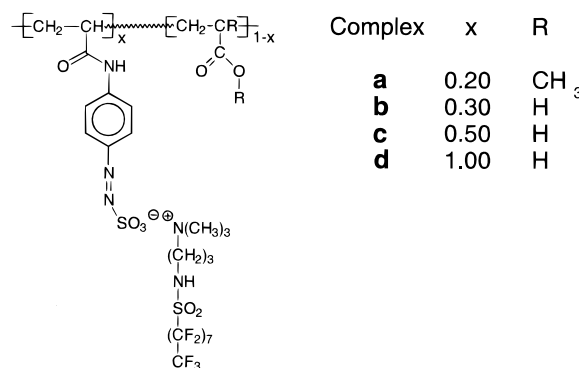


Figure 1. Complexes of poly[(acrylamidophenyldiazosulfonate)-*co*-(methacrylate)] (**a**) and poly[(acrylic acid)-*co*-(acrylamidophenyldiazosulfonate)] (**b–d**).

purified by passing them through a basic aluminum oxide column to remove the stabilizer and were then distilled. Fluorad FC-135 (3M) is a cationic fluorinated surfactant with a pendant perfluorinated alkyl chain of eight carbon atoms: (3-((heptadecafluorooctyl)sulfonyl)amino)propyl)trimethylammonium iodide. Fluorad FC-135 is commonly used as an active spreading agent and has a high affinity to numerous metals and silicon containing surfaces.¹⁰ 2,2,2-Trifluoroethanol (Aldrich, 99.5%) was used as a solvent for the complexes.

Synthesis of Polyelectrolytes. All free radical polymerizations were carried out in a 10% aqueous solution at 70 °C for a period of 17 h. The preparation of **Pa** (used for the preparation of complex **a**) by free radical copolymerization at 70 °C was similar to the procedure described earlier.⁸ For **Pa**, 5.1 mmol (1.5 g) of **M** and 20.0 mmol (2.0 g) of methyl methacrylate were polymerized using 0.62 mmol (0.103 g) of 2,2'-azobis(isobutyronitrile) in a dioxane/water (4/1 (v/v)) solution. Analysis of **Pa**: ¹H NMR (δ -DMSO, δ in ppm)¹ 0.6–1.2, 1.6–2.0, 3.5–3.7, 7.7–7.9 (H_{ar}); GPC M_n = 23 100 g/mol, M_w = 78 000 g/mol, M_w/M_n = 3.3. Polymer **Pb** (used for the preparation of complex **b**) was synthesized from 3.6 mmol (1.0 g) of **M** and 8.4 mmol (0.61 g) of acrylic acid similar to the synthesis of diazosulfonate polymers described earlier.⁸ The reaction was carried out in water with 0.63 mmol (0.18 g) of 4,4'-azobis(cyanovalelerianic acid) as initiator. **Pc** (used for the preparation of complex **c**) and **Pd** (used for the preparation of

* Corresponding author. E-mail: andreas.thuenemann@mpikg-golm.mpg.de.

[†] Max Planck Institute of Colloids and Interfaces.

[‡] Technische Universität München.

[§] Institut für Polymerforschung Dresden.

^{||} Heinrich Heine University Düsseldorf.

complex **d**) were prepared under the same conditions from 5.4 mmol (1.5 g) of **M** and 5.4 mmol (0.38 g) of acrylic acid and 0.57 mmol (0.16 g) of 4,4'-azobis(cyanovaleric acid) and from 7.2 mmol of **M** with 0.36 mmol (0.101 g) of 4,4'-azobis(cyanovaleric acid) as initiator. The polyelectrolytes were purified by dialysis in water. After evaporation of the water they were dried for 24 h in a vacuum at 50 °C. The yields were 1.5 g (94%, **Pb**), 1.7 g (89%, **Pc**), and 1.8 g (82%, **Pd**). Analysis of **Pb**: ^1H NMR (D_2O , δ in ppm) 1.1–3.0, 6.9–8.0; GPC M_n = 8900 g/mol, M_w = 10 200 g/mol, M_w/M_n = 1.15. Analysis of **Pc**: ^1H NMR (D_2O , δ in ppm) 1.1–3.0, 7.0–8.0; GPC M_n = 6750 g/mol, M_w = 7600 g/mol, M_w/M_n = 1.12. Analysis of **Pd**: ^1H NMR (D_2O , δ in ppm) 1.0–3.2, 5.7–8.3; GPC M_n = 6800 g/mol, M_w = 8200 g/mol, M_w/M_n = 1.20. The thermal behavior of the polyelectrolytes **Pa**, **Pb**, **Pc**, and **Pd** was determined by DSC measurements. The decomposition of the diazosulfonate functions started above 190 °C, and had a maximum decomposition rate between 220 and 230 °C. In the UV/vis spectra of the copolymers an intensive absorption with a maximum at 331 nm was found which corresponds to the diazosulfonate group.

Preparation of Complexes. A solution of 0.2 g polyelectrolyte in 20 mL of water was stirred at room temperature, and 1.0 equiv of the fluorinated surfactant Fluorad FC-135 (dissolved in 20 mL of water) was added in droplets (the stoichiometry was calculated according to the charges). The solid polyelectrolyte-surfactant complexes were precipitated after combining the two solutions and were obtained as yellow to brown precipitates. A pH value of 5, present at preparation, was adjusted using 0.1 N NaOH. The complexes were isolated, washed three times with 100 mL of water, and dried for 24 h. The yields were in the range 70–80%. The complexes were dissolved in 2,2,2-trifluoroethanol and cast into aluminum molds coated with Teflon. After the evaporation of the solvent, the films of the complex could be easily removed from the mold. Complex solutions of 0.1% (w/w) in 2,2,2-trifluoroethanol were used for the preparation of thin films. Silicon wafers with native oxide served as substrates. The complex was deposited onto the wafers using the spin-coat technique at a speed of 2000 rpm.

Measurements. Differential scanning calorimetry (DSC) measurements were made with a Netzsch DSC 200. The samples were examined at a scanning rate of 10 K/min by applying one cooling and two heating scans. Thermogravimetric analysis (TGA) was performed in a nitrogen atmosphere and with a heating rate of 10 K/min using a Netzsch TG 209 instrument. Wide-angle X-ray scattering (WAXS) measurements were carried out with a Nonius PDS120 powder diffractometer using transmission geometry. A FR590 generator was used as the source of Cu K α radiation. Monochromatization of the primary beam was achieved by means of a curved Ge crystal, and the scattered radiation was measured with a Nonius CPS120 position sensitive detector. The resolution of this detector in 2θ is about 0.018°. We performed the small-angle X-ray scattering experiments with a Kratky compact camera (Anton Paar), equipped with a stepping motor and a counting tube with an impulse-height discriminator. The light source was a conventional X-ray tube with a fixed copper target operating at 40 mA and 30 kV. The X-ray reflectivity was performed with a $\theta/2\theta$ instrument (Sot/Superman DF4, U = 40 kV, I = 30 mA, λ = 0.154 nm). The beam divergence of the incoming beam was 0.1 deg, the resolution in 2θ was 0.05 deg. A secondary monochromator selected the Cu K α lines, a scintillation counter served as detector. The surface compositions were measured using X-ray photoelectron spectroscopy (XPS) on a ESCALab 220I (Vacuum Generator, UK) with a Mg K α X-ray source (1253.6 eV photons). The X-ray source was run at a power of 300 W (15 kV, 20 mA). A CAE analyzer was used with pass energies of 80 eV for survey spectra and 25 eV for the high-resolution spectra. Surface chemical compositions were determined from the peak area ratios corrected with Wagner's sensitivity factors¹¹ and the spectrometer transmission function. Contact angle measurements were performed on a Krüss G10 contact angle goniometer. The angles reported here are the average of five measurements. The advancing

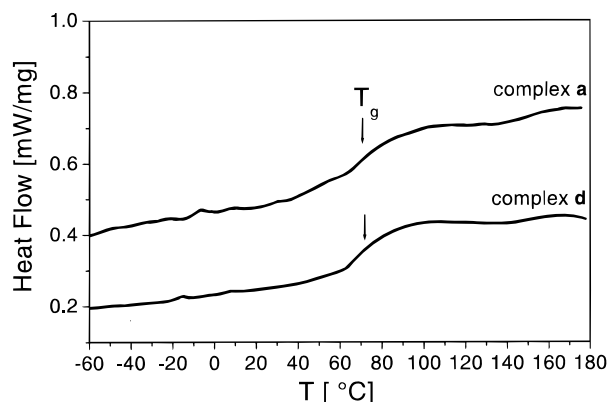


Figure 2. DSC thermograms of the complexes of **a** and **d** during heating (second heating cycle).

contact angle was determined by injecting a 5 μL liquid droplet, the receding contact angle was measured by removing about 3 μL of liquid from the droplet, and the static contact angle was obtained from a droplet (ca. 5 μL) on the surface. Linear alkanes and water (passed through MilliPore purification systems) were used as test liquids.

Results and Discussion

It is well-known that mixing equimolar amounts of water solutions of polyelectrolyte chain units and surfactants results in water insoluble complexes of stoichiometric complexes.^{3,12} In our experiments, mixing equimolar amounts of polyelectrolyte (see Figure 1, structures **a–d**) and a fluorinated surfactant resulted in complexes which precipitated immediately. After purification by washing with water, the complexes were dried in a vacuum, subsequently dissolved in trifluoroethanol and cast onto wafers to form transparent films.

Thermal Analysis. The thermal behavior of the complexes was investigated by DSC and TGA. Typical DSC thermograms are shown in Figure 2. It was found that all the complexes show glass transitions at 71 ± 3 °C. This result is somewhat surprising because one would have expected the glass transition to depend on the composition of the polymer. But obviously this is not the case, or if it is, the effect is too small to measure. Probably the reason for this is that the influence on the glass transition resulting from the surfactant is considerably stronger than that of the polymeric backbone. Support for this assumption comes from the fact that glass transitions around 30 °C were found for complexes of the same type of polymer, but with a different surfactant.⁸ In contrast, the absence of glass transitions is typical for noncomplexed polyelectrolytes because of their saltlike character. In accordance with these general properties of polyelectrolytes, no glass transitions were found for the pristine diazosulfonate polymers before decomposition of the azo groups took place. Above the glass transition of all complexes, no further thermal transitions were detected. From this we conclude that the complex is stable up to temperatures of about 180 °C. TGA measurements show that no significant weight loss of any of the complexes can be obtained below 180 °C, which confirms the DSC results. The TGA curves of complexes **a** and **d** are shown in Figure 3 (dashed and solid lines, respectively). It can be seen there that significant decomposition starts above 200 °C, and further, that the maximum decomposition rate of the complexes occurs in the range 230–240 °C. It was found that the complexes with higher charge densities are

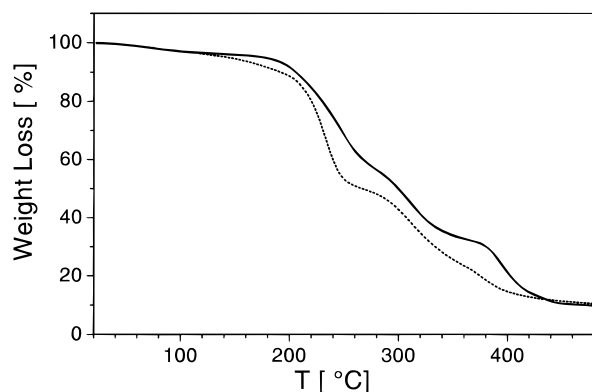


Figure 3. Thermograms of complex **a** (dashed line) and complex **d** (solid line).

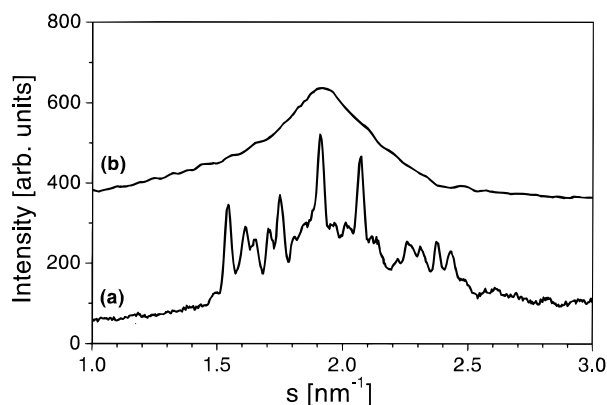


Figure 4. Wide-angle X-ray scattering diagrams of the surfactant (curve **a**) and complex **c** (curve **b**).

slightly more stable than the complexes with lower charge densities. The decomposition process was regarded as the thermal decomposition of the azo groups. This assumption was supported by an investigation of the thermal decomposition of diazosulfonate containing polymers and diazosulfonate containing surfactants.¹³ Therefore, we conclude that the thermal stability of the complexes is predominantly determined by the stability of the polymer.

Structure in the Bulk Material. The molecular and supramolecular structures of the complexes were examined using wide- and small-angle X-ray scattering experiments. In the wide-angle scattering diagram of all complexes one single broad peak was found (see Figure 4, upper curve). The peak maxima of all complexes correspond to a Bragg spacing of 0.52 nm. This can be attributed to the amorphous packing of the fluorinated chains (C_8F_{17}) in powder as well as in film samples, which is similar to the packing of shorter chains (C_6F_{13}) in complexes investigated earlier.⁸ In contrast a number of sharp reflections were found in the wide-angle diagram of the pure surfactant (Figure 4, lower curve), which proves that it is a crystalline material. As described for different types of complexes earlier, we conclude that the crystallization of the surfactant can be strongly reduced as a result of the complexation. The reason for this is that any movement of the surfactant in the complex is accompanied by a rearrangement of the polymeric backbone via the ionic bonds. In an earlier study we found that a high charge density and a C_9F_{19} chain of the fluorinated moieties is necessary to produce a side-chain crystalline structure in the complex. In a number of studies it was shown that numerous PEFAs are characterized in particular

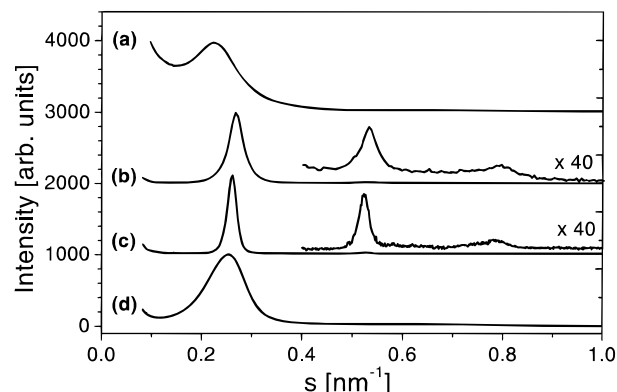


Figure 5. Small-angle X-ray scattering of complexes **a–d**. Powder samples were used. The magnification of the inserts is 40 (complexes **c** and **d**).

by their mesomorphous structures.⁵ The presence of more or less sharp reflections in the small-angle-scattering curves of the complexes proves that the charge density of all diazosulfonate polymers is sufficiently high for the formation of mesomorphous ordered structures. This confirms the results from an earlier work where it was found that a charge density of about 25% was necessary to form ordered complex structures.¹⁴ It can be seen in Figure 5 that the width of the most intense reflection is lower for the complexes of medium charge densities (**b**, **c**) than it is for the complexes with either a low or high charge density (**a** and **d**, respectively). For the former reflections of a higher order are present with relative positions of 1:2:3. Together with the results from the wide-angle scattering and the DSC, we can conclude that the complexes are isomorphous with a lamellar structure of a smectic A type. The structures are similar to those of the fluorinated polymers reported by Ober et al.³⁰ From the reflex positions, the long periods were determined to be 4.4 (**a**), 3.8 (**b**), 3.9 (**c**), and 4.0 nm (**d**). This is in agreement with a multilayer structure of alternating fluorinated and ionic sheets. The former contain the fluorinated surfactant tails and the latter are enriched with the polyelectrolyte chains and the ionic headgroups. From the integral width of the first-order reflection, the correlation lengths^{15,16} of the complexes were determined to be 10 (**a**), 30 (**b**), 45 (**c**), and 11 nm (**d**). Obviously complexes **b** and **c**, which have medium charge densities of 30 and 50%, are better ordered than the complexes with the lowest and highest charge densities (**a** and **d**). Probably the steric constraints within the structure of the complexes are reduced to an optimum at a charge density of about 50 mol % diazo-sulfonate groups.

Ultrathin Films. Thin complex films on silicon wafers were prepared by the spin-coat technique from complex solutions and investigated by X-ray reflectivity. Examples of reflectivity curves of ultrathin films are shown in Figure 6. Well-defined double-layer stacks were developed within a few seconds simply as a result of the deposition of droplets of the complex solution. It was found that complex **c**, which has the highest correlation length in the bulk material, forms the best ordered films. In Figure 6a, the presence of Kiessig fringes indicate a smooth complex film. A thickness of 4.0 ± 0.5 nm was calculated from the angular position of the fringes.¹⁷ In the diagrams of films of larger thickness, three equidistant Bragg peaks appear. The peak positions result in lamellar spacings which are

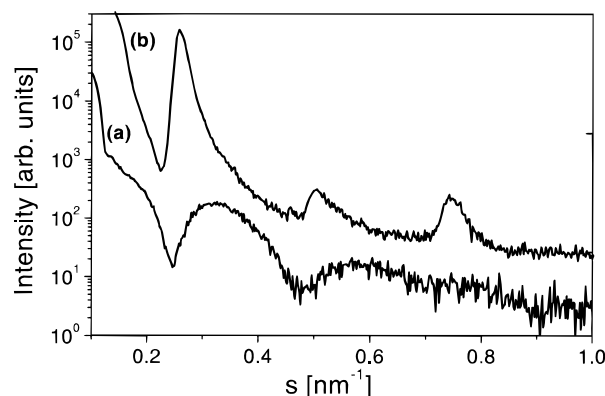


Figure 6. X-ray reflectivity curves of thin films of complex **b** on silicon wafer surfaces. The film thicknesses are 4 nm (curve a) and about 40 nm (curve b).

Table 1. XPS Data for Complex Coated Silicon Wafers

com- plex	exit angle, deg	atom %									
		experimental					theory ^a				
		C	F	N	O	S	C	F	N	O	S
a	90	45.1	28.6	4.9	17.9	3.5	53.1	20.9	6.2	17.3	2.5
	45	38.2	41.4	4.1	13.4	2.9					
b	90	47.0	33.4	5.7	11.8	2.1	46.4	26.3	7.7	16.5	3.1
	45	38.9	43.0	4.6	11.0	2.5					
c	90	44.7	33.4	5.7	13.7	2.5	44.8	29.3	8.6	13.8	3.5
	45	39.2	42.4	4.6	11.3	2.5					
d	90	37.4	46.2	4.7	9.0	2.7	43.4	32.1	9.4	11.3	3.8
	45										

^a Values represent the bulk composition of a stoichiometric complex according to Figure 1.

equal, or slightly larger, than that of the complexes in the materials in bulk form. As an example, Figure 6b shows the scattering curve of a film of complex **c** with a lamellar spacing of 4.0 nm and a correlation length between 36 and 40 nm. Because of the same mesomorphic structure was developed in a slow film forming process (solvent casting) and in a fast film forming process (spin coating), we conclude that the time which is necessary for the formation of the mesophase is shorter than the time necessary for the formation of the films. The latter is in the order of one second. The structure of a film producing a scattering curve such as in Figure 6b can be explained as consisting of multilayers aligned parallel to the wafer surface. In a recent study on model systems of low friction polymer coatings, we described in detail the macroscopic orientation of complexes to multilayers with a variability of about two decades in thicknesses.³⁴ Such polymer multilayer, produced in a single-step procedure, seem to be of interest in the formation of self-assembled organic multilayer films.

To determine the elemental composition at the film surfaces, xps measurements were carried out. In this surface spectroscopic experiment, the sample of interest was irradiated with a Mg K α X-ray. The kinetic energy of the emitted photoelectron was recorded. Since the mean free path of the ejected photoelectron controls the analysis depth, an analysis of the outer 5 nm of the polymeric surface can be obtained by changing the angle of the sample surface relative to the collection aperture of the spectrometer. The complex coated silicon wafers were examined using this approach and they were compared with the average complex composition in the bulk material. The results are shown in Table 1. It can be seen there that the fluorine content at the surface of all the complexes is higher than the calculated average

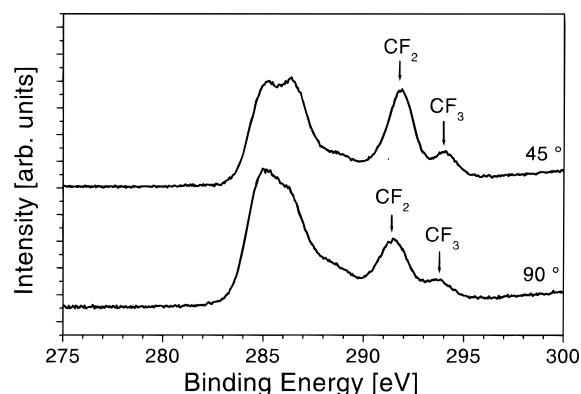


Figure 7. XPS carbon 1s core-level spectra of complex **b** films on silicon wafer. The takeoff angles are 90 (lower curve) and 45° (upper curve).

bulk composition. Furthermore, the fluorine content depends strongly on the takeoff angle. At the lower takeoff angle of 45°, which corresponds to the lower sampling depth of roughly 3 nm, the detected amount of fluorine increases from 41 to 46 atom % in the line from complex **a** to **d**. These values are significantly higher than the average values of the fluorine content of the complexes, which increase from 21 to 32 atom %, and indicate an enrichment of the fluorine groups at the complex surfaces. High-resolution spectra were collected in the region of the carbon 1s in order to estimate the CF₂/CF₃ ratios. Typical examples for takeoff angles of 90 and 45° are given in Figure 7 for complex **b**. The takeoff angle is defined as the angle between the sample surface and the detector. Discrete peaks at binding energies of 292 and 294 eV were assigned to the CF₂ and CF₃ functional groups, and show clearly the -(CF₂)₇-CF₃ chains at the air/complex interface. The ratios of the CF₃ to CF₂ groups are about 0.24 and 0.35 for takeoff angles of 90 and 45°, respectively. Both values are significantly higher than the value calculated for the average composition (0.14). This confirms the assumption that the fluorinated chains are oriented toward the air/complex surface. It was found that the polymer complexes decompose significantly when irradiated with a Mg K α X-ray in a high vacuum during the xps measurements. Therefore, it was not possible to perform angle-dependent high-resolution measurements of high accuracy in order to determine the differences of the complexes in respect to their enrichment of CF₃ groups at the surface. The radiation-induced decomposition of fluorinated polymers is well-known, for example, in the XPS investigation of perfluorinated polyethers¹⁸ and is not a characteristic property of fluorinated polymer complexes. An indirect method, which supplies information about the surface composition, is the determination of the surface energy by contact angle measurements.

Surface Energies. Films of complexes **a–d**, prepared by solvent casting and by spin coating, were investigated by using dynamic contact angle measurements with an automatic axisymmetric drop shape analysis.^{19,20} The results are summarized in Table 2. It was found in particular that all nonpolar liquids, which spread readily on uncoated surfaces, showed high contact angles on complex-coated surfaces. In addition, no significant difference was found between the contact angles of solvent cast films and spin coat films. This observation is in agreement with our interpretation, namely that the structure formation of the complexes

Table 2. List of Contact Angles of Different Solvents on Glass Surfaces Coated with Complex Solutions at 20 °C, Where the Surface Tensions of the Test Liquids, Advancing, Stationary, and Receding Contact Angles Measured by a Krüss Contact Angle Goniometer Are Listed, and the Surface Tensions of the Complex Surfaces γ Were Calculated Using the Equation of Neumann and Li (Eq 1)

solvent	surface tension (mN/m)	advancing angle (deg) ^a	stationary angle (deg) ^a	receding angle (deg) ^a	γ (mN/m)
Complex a					
hexane	18.4	49	48	40	12.7
octane	21.8	60	59	50	12.5
decane	23.9	64	62	48	12.8
dodecane	25.4	68	60	50	12.5
hexadecane	27.6	72	70	52	12.5
water	72.7	74	71	<i>b</i>	39.2
Complex b					
hexane	18.4	55	52	39	11.5
octane	21.8	61	56	44	12.3
decane	23.9	67	63	45	12.0
dodecane	25.4	76	72	46	10.3
hexadecane	27.6	79	75	49	10.5
water	72.7	100	97	<i>b</i>	23.0
Complex c					
hexane	18.4	56	53	44	11.3
octane	21.8	65	58	51	11.3
decane	23.9	70	66	56	11.2
dodecane	25.4	76	70	56	10.3
hexadecane	27.6	79	74	61	10.5
water	72.7	97	88	<i>b</i>	24.8
Complex d					
hexane	18.4	45	40	20	13.5
octane	21.8	53	51	21	14.2
decane	23.9	63	59	19	13.0
dodecane	25.4	65	63	25	13.3
hexadecane	27.6	70	69	34	13.1
water	72.7	84	75	<i>b</i>	32.9

^a Error of measurement ca. 1°. ^b Receding angles are erratic.

is faster than the film forming process in the procedures used. However, direct measurement of the surface energies of nonelastomeric solid materials is not simple. For practical reasons, procedures based on contact angle measurements are normally used.^{21–27} Neumann and Li derived an equation, by which it is possible to calculate the surface free energy of a solid,²⁸ such that

$$\cos \theta = -1 + 2 \sqrt{\frac{\gamma_s}{\gamma_1}} \exp(-\beta(\gamma_1 - \gamma_s)^2) \quad (1)$$

where β is a constant ($1.247 \times 10^{-4} \text{ m}^2 \text{ mJ}^{-1}$). Thus, the surface energy γ_s can be determined from the experimental contact angles and the liquid surface tension γ_1 . The surface energies were calculated using eq 1 range from 10.3 to 14.2 mN/m for the homologue series of alkanes used as test liquids with surface tensions in the range 18.4–27.6 mN/m (Table 2). These values are of the same order of magnitude as the surface energies found in fluorinated polymer- (FC-725) coated silicon wafers.²⁷ These range from 10.3 to 13.1 mN/m. It was found that the complexes with the higher supramolecular ordering (**b** and **c**) possess lower surface energies than the complexes with the lower ordering (**a** and **d**). This is probably due to the influence of the lamellar ordering within the bulk material on the alignment of the CF_3 groups at the air/complex interface. The critical surface tension γ_c of a surface can often be determined by the contact angles of a homologue

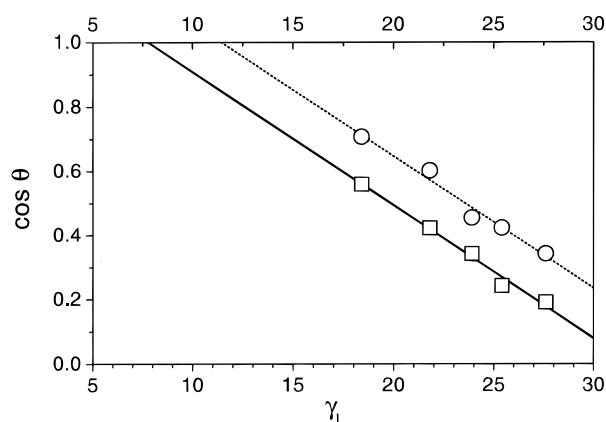


Figure 8. Zisman plots for complex coated glass surfaces. Points are obtained with (1) hexane, $\gamma_1 = 18.4 \text{ mN/m}$; (2) octane, $\gamma_1 = 21.8 \text{ mN/m}$; (3) decane, $\gamma_1 = 23.9 \text{ mN/m}$; (4) dodecane, $\gamma_1 = 25.4 \text{ mN/m}$; and (5) hexadecane, $\gamma_1 = 27.6 \text{ mN/m}$. The critical surface tension of complex **c** was calculated to be 7.8 mN/m by extrapolating a linear fit (solid line) of the $\cos \theta$ (squares) to $\cos \theta = 1$. For complex **d** (circles), a critical surface tension of 11.4 mN/m was determined (dotted line). Advancing contact angles were used for $\cos \theta$.

Table 3. Zisman Critical Surface Energies γ_c and the Dispersive Surface Energies γ_s^d According to the Girifalco–Fowkes–Young Equation of Complex Films on Glass

complex	γ_c (mN/m)	γ_s^d (mN/m)
a	8.9 ± 0.9	12.2 ± 0.1
b	6.9 ± 1.2	11.4 ± 0.2
c	7.8 ± 1.0	10.6 ± 0.3
d	11.4 ± 1.6	13.1 ± 0.3

series of nonpolar liquids.²¹ γ_c defines the wettability of a solid by fixing the lowest surface tension a liquid can have and still exhibit a contact angle greater than zero degrees. The γ_c value of a surface is usually obtained from a Zisman plot of the contact angles;²¹ such a plot of $\cos \theta$ against the surface tensions of liquids (γ_1) is a straight line with the slope m :

$$\cos \theta = 1 + m(\gamma_1 - \gamma_c) \quad (2)$$

The extrapolation of γ_1 to $\cos \theta = 1$ gives γ_c . Zisman plots (see Figure 8 and Table 3) result in critical surface tensions of 6.9 (complex **b**) to 11.4 mN/m (complex **d**). Within the observed experimental error, the values of complexes **b** and **c** are close to an oriented close-packed monolayer of perfluorododecanoic acid (6 mN/m), which forms the lowest surface energy known to date.²⁹ As recently demonstrated by Ober et al.,³⁰ such surface energies are typically found in fluorinated side group block copolymers in the smectic A phase. Therefore, together with the X-ray results, the complexes are similar to a smectic A side chain polymer. In contrast, the fluorinated chains are not bound covalently but ionically. Considering the critical surface energy data and the results from the xps measurements, we conclude that the complex surfaces were strongly enriched with close-packed $-\text{CF}_3$ groups. It must be stressed here that although γ_c values are widely used for surface characterization, there is no theoretical justification for equating the critical surface tension with the surface energy of a material. The wettability data were also used to determine the dispersion force component of the surface energy γ_s^d by using the Girifalco–Good–

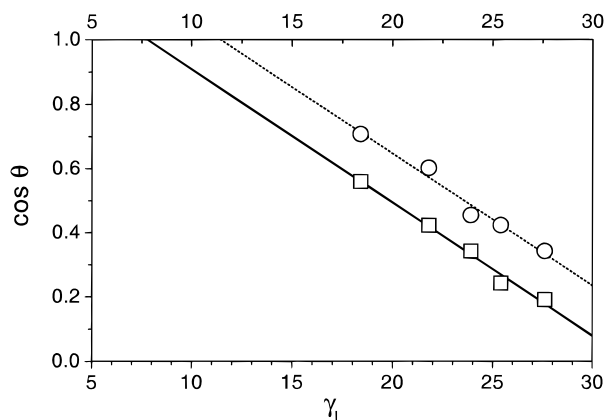


Figure 9. Girifalco–Good–Fowkes–Young plots for the determination of the dispersive surface energy of complex coated glass surfaces. From left to right the points are values obtained with (1) hexadecane, $\gamma_l = 27.6$ mN/m; (2) dodecane, $\gamma_l = 25.4$ mN/m; (3) decane, $\gamma_l = 23.9$ mN/m; (4) octane, $\gamma_l = 21.8$ mN/m; and (5) hexane $\gamma_l = 18.4$ mN/m. The γ_s^d values were calculated from the slope to be 12.2 mN/m for complex **a** (squares represent measured angles and the solid line the least-squares fit) and 13.1 mN/m for complex **d** (circles, dotted line).

Fowkes–Young equation,^{22,23} which has the form

$$\cos \theta = -1 + 2 \sqrt{\frac{\gamma_s^d}{\gamma_l}} \quad (3)$$

This equation is fitted to the plot of $\cos \theta$ against $(1/\gamma_l)^{1/2}$ for dispersive liquids with the ordinate of the best linear fit located at -1 , the gradient being $2(\gamma_s^d)^{1/2}$. The Girifalco–Good–Fowkes–Young plots are used to determine γ_s^d (Figure 9). Linear fits result in dispersive surface energies of $\gamma_s^d = 12.2 \pm 0.1$ mN/m (complex **a**), 11.4 ± 0.2 mN/m (complex **b**), 10.6 ± 0.3 mN/m (complex **c**), and 13.1 ± 0.3 mN/m (complex **d**). All results are summarized in Table 3. These values are slightly higher than those found for a highly fluorinated side-chain styrene (9.3 mN/m²⁵) and some other fluorinated polyelectrolyte–surfactant complexes.^{31,32} However, the γ_c and γ_s^d values indicate a high enrichment of the CF_3 groups on the complex surface. It is particularly interesting that the contact angles of water (the most polar test liquid with $\gamma_l = 72.7$ mN/m) are relatively low. Again, the surface energies calculated using the eq 1 are higher for the complexes with the lower degrees of order in the bulk material (39.2 (**a**) and 32.9 mN/m (**d**)) than for the complexes with the higher degrees of order (23.0 (**b**) and 24.8 mN/m (**c**)).

The low surface energies determined for nonpolar liquids were reproduced, even when the complex coated surfaces were dried after exposure to water. This indicates a reversible surface reconstruction of the complex surface after it has been in contact with water. Surface reconstruction phenomena are widespread in polymer coatings, such as self-organizing semifluorinated side-chain ionenes²⁶ and even polymers containing only a few polar groups such as Teflon–PFA.³³ It is worth noting that the surface reconstruction of the complex when in contact with water, seems to be very fast, as shown by the static constant contact angle of water which adjusts to an equilibrium within a few seconds. The degree and speed of surface reconstruction is assumed to be dependent on several factors, such as the number of polar groups within a distance of about

1 nm from the surface. Taking into account the correlation lengths, there seems to be an optimum at a content of about 30–50 mol % of charged monomers in forming low energy surfaces and in forming ordered structures. Thin coatings of the complexes seem to be promising for the development of surfaces, which can be switched irreversible from an ultralow energy surface to a high energy surface by using a laser beam.

Conclusion

We have shown that the lamellar solid-state structures of water-insoluble complexes of diazosulfonate-containing polyelectrolyte fluorosurfactant complexes are formed in the bulk material and in thin films. The correlation length of the complexes and the surface energies of complex coated surfaces were tuned by the charge density of the polyelectrolyte. In contrast the glass-transition temperature was found to be independent of the degree of charged monomers. All complexes are thermally stable up to temperatures around 200 °C and display similar thermal decomposition behavior.

Acknowledgment. We wish to thank C. Remde for help in measuring the contact angles, Dr. Simon for the XPS analysis, and S. Kubowicz for performing the X-ray reflectivity measurements. Financial support of the German Science Foundation (Grant Lo418/7-1) and the Max-Planck Society is gratefully acknowledged.

References and Notes

- (1) Ober, C. K.; Wegner, G. *Macromolecules* **1997**, *9*, 117.
- (2) Antonietti, M.; Henke, S.; Thünemann, A. F. *Adv. Mater.* **1996**, *8*, 41–45.
- (3) Ponomarenko, E. A.; Tirrell, D. A.; Macknight, W. J. *Macromolecules* **1998**, *31*, 1584–1589.
- (4) Ponomarenko, E. A.; Tirrell, D. A.; Macknight, W. J. *Macromolecules* **1996**, *29*, 8751–8758.
- (5) Thünemann, A. F. *Polym. Int.* in press.
- (6) Products are on the market which form easy-to-clean surfaces. An example is the protection of walls from graffiti. Products with low friction are used for ski and biathlon sports. Information supplied by Colloid Surface Technologies GmbH, Wiesbaden, Germany (www.cerax.de).
- (7) Antonietti, A.; Kublickas, R.; Nuyken, O.; Voit, B. *Macromolecular Rapid Communication* **1997**, *18*, 287–294.
- (8) Thünemann, A. F.; Schnöller, U.; Nuyken, O.; Voit, B. *Macromolecules* **1999**, *32*, 7414–7421.
- (9) Matusche, P.; Nuyken, O.; Voit, B.; Van Damme, M.; Vermeersch, J.; De Winter, W.; Alaerts, L. *React. Polym.* **1995**, *24*, 271–278.
- (10) Information supplied by the manufacturer, Hoechst AG, Frankfurt, Germany.
- (11) Wagner, C. D.; Davis, L. E.; Zeller, M. W.; Taylor, J. A.; Raymond, R. H.; Gale, L. H. *Surface Interface Anal.* **1981**, *3*, 211–225.
- (12) Goddard, E. D.; Ananthapadmanabhan, K. P. *Interactions of Surfactants with Polymers and Proteins*; CRC Press: Boca Raton, FL, 1993.
- (13) Stasko, A.; Erentova, K.; Rapt, P.; Nuyken, O.; Voit, B. *Magn. Reson. Chem.* **1998**, *36*, 13–34.
- (14) Thünemann, A. F.; Lochhaas, K. H. *Langmuir* **1998**, *14*, 4898–4903.
- (15) Scherrer, P. *Gött. Nachr.* **1918**, *2*, 98.
- (16) Klug, H. P.; Alexander, L. E. In *X-ray Diffraction Procedures for Polycrystalline and Amorphous Materials*; Wiley: New York, 1974; p 487.
- (17) Holy, V.; Pietsch, U.; Baumbach, T. In *High-Resolution X-ray Scattering from Thin Films and Multilayers*; Springer Tracts in Modern Physics 149; Springer: Berlin 1999.
- (18) Pan, F. M.; Lin, Y. L.; Horng, S. R. *Appl. Surf. Sci.* **1991**, *47*, 9–16.

- (19) Augsburger, A.; Grundke, K.; Pöschel, K.; Jacobasch, H.-J.; Neumann, A. W. *Acta Polym.* **1998**, *49*, 417426.
- (20) Kwok, D. Y.; Neumann, A. W. *Adv. Colloid Interface Sci.* **1999**, *81*, 167–249.
- (21) Zisman, W. A. *Ind. Eng. Chem.* **1963**, *55*, 18.
- (22) Fowkes, F. M. *J. Phys. Chem.* **1962**, *66*, 382.
- (23) Girifalco, L. A.; Good, R. J. *J. Phys. Chem.* **1957**, *61*, 904.
- (24) Drummond, C. J.; Georgaklis, G.; Chan, D. Y. C. *Langmuir* **1996**, *11*, 2617–2621.
- (25) Höpken, J.; Möller, M. *Macromolecules* **1992**, *25*, 1461–1467.
- (26) Wang, J.; Ober, C. K. *Macromolecules* **1997**, *30*, 7560–7567.
- (27) Kwok, D. Y.; Lam, C. N. C.; Li, A.; Leung, A.; Wu, R.; Mok, E.; Neumann, A. W. *Colloids Surf.* **1998**, *142*, 219–235.
- (28) Li, D.; Neumann, A. W. *J. Colloid Interface Sci.* **1992**, *148*, 190–200.
- (29) Hare, E. F.; Shafring, E. G.; Zisman, W. A. *J. Colloid Sci.* **1954**, *58*, 236–239.
- (30) Wang, J.; Mao G.; Ober, C. K.; Kramer, E. J. *Macromolecules* **1997**, *30*, 1906–1914.
- (31) Thünemann, A. F.; Lieske, A.; Paulke, B. R. *Adv. Mater.* **1999**, *11*, 321–324.
- (32) Thünemann, A. F.; Lochhaas, K. H. *Langmuir* **1999**, *15*, 4867–4874.
- (33) Yasuda, H.; Okuno, T.; Sawa, Y.; Yasuda, T. *Langmuir* **1995**, *11*, 3255–3260.
- (34) Thünemann, A. F.; Kubowicz, S.; Pietsch, U. *Langmuir*, in press.

MA000216L